Optimization of compressed stiffened flanges in bridge box girder cross section

Authors:

Assist.Prof. **Anđelko Vlašić**, PhD. CE
University of Zagreb
Faculty of Civil Engineering
vlasic@grad.hr

Nijaz Mujkanović, MSc. CE
University of Zagreb
Faculty of Civil Engineering
nijaz@grad.hr

Subject review

Anđelko Vlašić, Nijaz Mujkanović

Optimization of compressed stiffened flanges in bridge box girder cross section

Due to bending, flanges of steel box girder cross sections act as compression plates and require stiffeners. Using stability evidence from EN 1993-1-5, a parametric study was performed for six different types of stiffeners. The obtained diagrams show design buckling resistance stress for various plate width and thickness values, and the type and number of stiffeners. Furthermore, an optimization process was performed to find the most suitable types and number of stiffeners, depending on the acting design compression force. Optimization parameters are the minimum steel area and minimum number of stiffeners.

Key words:

bridge, steel box, compression flange, buckling, stiffening, reduced stress method

Pregledni rad

Anđelko Vlašić, Nijaz Mujkanović

Optimizacija ukrućenih tlačnih pojasnica u sandučastom presjeku mosta

Uslijed savijanja, pojasnice čeličnih sandučastih presjeka grednih mostova ponašaju se kao tlačni pločasti elementi i zahtijevaju ukrućenja. Koristeći dokaz stabilnosti prema EN 1993-1-5 provedena je parametarska analiza za 6 različitih tipova ukrućenja. Dobiveni dijagrami pokazuju računsko naprezanje otpornosti na izbočivanje za različite širine i debljine ploča, te tip i broj ukrućenja. Nadalje, proveden je optimizacijski postupak kojim se pronalazi najpovoljniji tip i broj rebara ovisno o djelujućoj računskoj tlačnoj sili. Optimizacijski parametri su minimalna površina čelika i minimalni broj rebara.

Ključne riječi:

most, čelični sanduk, tlačni pojas, stabilnost, izbočivanje, ukrućenje, metoda smanjenog naprezanja

Übersichtsarbeit

Anđelko Vlašić, Nijaz Mujkanović

Optimierung ausgesteifter Druckflanschen kastenförmiger Brückenquerschnitte

Bei Biegung verhalten sich Flanschen kastenförmiger Stahlquerschnitte von Balkenbrücken wie Druckplattenelemente und erfordern Aussteifungen. Dem Stabilitätsnachweis gemäß EN 1993-1-5 folgend wurde eine Parameteranalyse für sechs Aussteifungstypen durchgeführt. Die resultierenden Diagramme zeigen Bemessungswerte des Knickwiderstands für verschiedene Plattenbreiten und –stärken, sowie Typ und Anzahl der Aussteifungen. Des Weiteren wurde ein Optimierungsverfahren durchgeführt, um in Abhängigkeit der einwirkenden Berechnungsdruckkraft den passenden Typ und die Anzahl der Aussteifungen zu ermitteln. Als Optimierungsparameter gelten eine minimale Stahlfläche sowie eine minimale Anzahl Rippen.

Schlüsselwörter:

Brücke, kastenförmiger Stahlquerschnitt, Druckband, Knicken, Aussteifung, Methode reduzierter Spannungen

1. Introduction

Many bridges comprise steel box cross sections subjected to bending. In the most common case the bridge superstructure is a continuous girder of medium to long span (typically ranging from 70 to 250 m in length). Flanges of such girders are compression and tension plates with stiffeners. The type and number of these stiffeners can differ for each design case significantly. In preparation for this research, a total of 14 real bridge projects were selected, all from Croatia, either already built or at the planning stage. All of them successfully passed the state revision process in the period from 2004 to 2015. Many discrepancies can be observed when examining the types of stiffeners with regard to plate thickness and stiffened width (Figure 1). No clear connection can be seen between these cases, when considering the reasons for selection of a particular type or number of stiffeners. Since most of these bridges were designed according to Eurocode, it can be concluded that the utilization of the stiffened compression plates differs to a great extent, which then affects the price of erection through steel consumption and workshop time.

Current research on the optimization of stiffened plates in bridges includes sections where only webs are stiffened with one stiffener, flanges are unstiffened, and the load is constant [1]. Also, continuous girder box section elements are optimised using search algorithms [2], but these section panels are not subjected to buckling due to small span and panel lengths. Plastic load bearing capacity for a composite open bridge section with web stiffeners subjected to buckling is also investigated [3] and recommendations are given not to fully utilize plastic

moment capacity in the mid span. During this research, compression of stiffened flanges at the support has not been investigated. Charts for design resistance of stiffened box girder flanges have been derived according to nonlinear analysis by the finite elements method, and the comparison is made with charts according to Eurocode design [4]. Other relevant research efforts concentrating on plate buckling propose buckling factors for webs without stiffeners comprising panels of variable thickness, depending on the aspect ratio, stress ratio, and panel thickness ratio of web plates [5].

The goal of the research presented in this paper is to optimize steel consumption in compressed stiffened plates acting as flanges in steel box girder bridges by choosing the best performing type and number of stiffeners, as related to the compression force and plate thickness. Buckling resistance is determined according to HRN EN 1993-1-5, Section 10, [6] using the reduced stress method recommended for use in bridges [7]. This method is used to determine a utilization factor for a stiffened plate given the acting ultimate limit stresses (see section 3.1). Assuming the utilization factor is 1.0 (full utilization), the largest design stresses for plate are calculated in this study and, consequently, the design compression force is determined, considering the area of the stiffened plate. Using these results, charts have been plotted that show, for each plate width and stiffener type, the required number of stiffeners, plate thickness, and the total steel area of the stiffened plate as related to compression force in the plate. By analysing these charts, an optimal stiffened plate can be chosen. Shear lag effects due to flange orthotropy are also considered through adequate reduction in flange steel area (effective width).

#	Bottom flange stiffner	Plate width / stiffner spacing Plate thickness	#	Bottom flange stiffner	Plate width / stiffner spacing Plate thickness	#	Bottom flange stiffner	Plate width / stiffner spacing Plate thickness
1		6000 / 800 $t_f = 30$	6		6600 / 1000 $t_f = 85$	11		6760 / 1300 $t_f = 80$ 8440 / 1300 $t_f = 60$
2		6300 / 800 $t_f = 25$	7		5700 / 600 $t_f = 40$	12		9000 / 1550 $t_f = 50$
3		7940 / 900 $t_f = 25$	8		6000 / 850 $t_f = 30$	13		3900 / 865 $t_f = 30$
4		9900 / 880 $t_f = 40$	9		4000 / 1150 $t_f = 50$	14		6300 / 1100 $t_f = 28$
5		9900 / 880 $t_f = 12$	10		5000 / 1000 $t_f = 16$			

Figure 1. Existing stiffeners for bottom flanges of bridge box sections

2. Scope of research

2.1. Bridge type, span length and cross section

Although the concept of this optimization method can be applied to any stiffened compression plate, some initial fixed variables influencing the buckling resistance calculation are set to best suit the cross section of box girder bridges. Compression plates analysed can be found in continuous steel box girders with the distance between webs (defining the plate width) ranging from 4 to 10 m (Figure 2).

Results can be applied only to bottom flanges where there are no additional local effects from vehicle axle loads, and the only acting load is a uniform compression force in longitudinal direction. However, the calculation of buckling resistance is not directly influenced by bridge span, since the shear lag effects are also taken into consideration (Section 4.1). It is recommended that the applied spans range between 70 and 250 m. This span range covers typical medium to long span steel and composite box girder bridges where effective lengths (L$_e$ from HRN EN 1993-1-5 3.2.1 [6]) for calculating the effective width of bottom compression flange are between 40 and 130 m. As long as effective lengths are within this range, the maximum error will be less than 4.37 %, which is considered acceptable (Section 4.1). Box girders in bridges are usually transversely stiffened against warping at every 4 m intervals. Also, when considering a cross section with an orthotropic deck plate, the distance between cross girders is typically also 4 m. This is why the buckling resistance is calculated with the length of the plate set to 4 m. Thus, one less variable is used for buckling verification. Material used in calculation is steel S355 which has the yield strength of f$_y$ = 355 MPa for the thickness of t ≤ 40 mm, and f$_y$ = 335 MPa for t ≤ 80 mm. Relevant standard HRN EN 1993-1-1 (Table 3.19) [8] allows for the application of this reduced number of classes for mechanical properties of hot rolled constructional steel. Constructional steel used for bridges of aforementioned spans rarely differs from S355 quality.

2.2. Types of stiffeners and plate thickness

Several types of stiffeners can be differentiated according to Figure 1. All these stiffeners are of closed section, which is nowadays almost exclusively used for compression plates in bridges. Open section stiffeners must be additionally checked for torsional buckling. Thus, conservatively, according to Section 9.2.2 from HRN EN 1993-1-5 [6], straight open-section stiffeners must fulfil the following condition:

$$\frac{I_T}{I_P} \geq 5,3 \frac{f_y}{E} \tag{1}$$

It is very difficult to fulfil this condition unless the stiffener is 20 mm or more in thickness. Similar requirements [9], which are also hard to fulfil, apply to other open section stiffeners with warping stiffness (T or Γ shaped). Because of these additional verifications, associated with open section stiffeners, and because such stiffeners are rarely used, they are not considered in this research. Other studies employing finite element solutions for T shaped stiffeners [10, 11], or analytical solutions [12], are also available.

Stiffener performance is mainly dictated by its height, which ranges from 240 mm to 490 mm for the existing bridges under study (Figure 1). Two main characteristics of stiffeners, the area and moment of inertia, are presented in Figure 3. Most of these stiffeners are between 240 mm and 300 mm in height, and their characteristics shown in the chart are quite similar. One of the objectives of this research was to group these different real stiffeners into several types according to their performances, and to suggest adding new ones to provide a larger scope for optimization. The lack of stiffeners higher than 490 mm would result in an incomplete analysis. Also, as this research will show (see interpretation in Section 4.3), stiffeners higher than 400 mm are very economical for very high box sections (possible heights of more than 10 m), and especially for box sections with wide lower flanges. Therefore, a total of 6 types were chosen with heights of 250, 300, 400, 500, 600 and 700 mm,
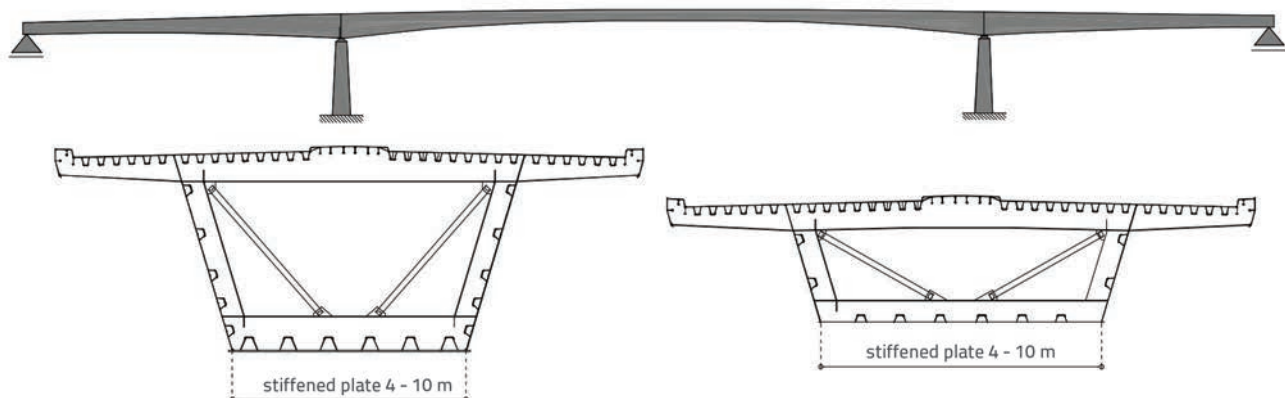

Figure 2. Examples of stiffened compression plates used in bridge sections

respectively, as shown in Figure 4. Their characteristics are also plotted and compared to real ones (Figure 3). For the design of the sections with trapezoid stiffeners, stiffener properties are derived by applying the straight web and flange axis geometry of the stiffener (numbers indicated along the axis lines in Figure 1 and Figure 4). It is standard practice to overlook a small loss due to radius of bending from web to flange when calculating static and design properties of the stiffeners [9]. The radius of r ≥ 2t is assumed (t is the thickness of the plate from which the stiffener is made) with minimum value of 20 mm (applicable to stiffeners 8 mm in thickness, less than that is avoided). The selection of material quality ensures that usual manufacturing techniques (bending and welding) do not compromise mechanical resistance and stability. For very "thick" stiffeners (where material thickness is t ≥ 12 mm), the recommended manufacturing method for single stiffeners involves longitudinal welding between the stiffener web and the stiffener flange. In this case, the difference of material with regard to properties calculation is even smaller.
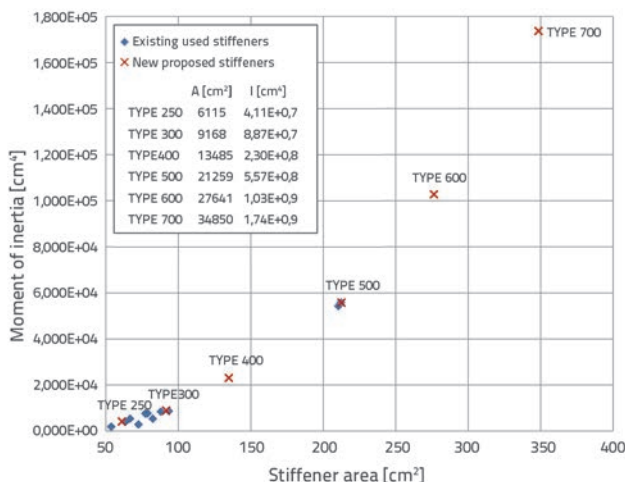

Figure 3. Stiffener properties – area and moment of inertia

Properties of Types 250, 300 and 500, shown in Figure 3, correspond very well to stiffeners from practice. Added Types 400, 600 and 700 will allow for a broader performance comparison given that their characteristics fill the missing gaps in the chart (Figure 3). The stiffener web to plate angle was set to 73° for all types. This value is somewhere in between the largest (81°) and the smallest (68°) angles observed in real stiffeners. With this value, the problem associated with small angles, where the stiffener flange is too narrow on higher stiffeners, is avoided, and so the moment of inertia of the stiffener is not unnecessarily reduced. Also, the angle is not too high as this would cause webs of the same stiffener to be too close to each other near the connection to the plate and, consequently, more stiffeners would be needed for the same plate width.

Stiffener thickness was chosen for each type according to class 3 condition $c/t ≤ 42\sqrt{(235/f_y)}$ or $c/t ≤ 34.2$ for f_y=355 MPa, ≥, which gives the smallest thickness of 8 mm for Type 250 stiffener and 20 mm for Type 700 stiffener (Figure 4). This condition was important because of the buckling verification performed according to the reduced stress method (HRN EN 1993-1-5, Section 10 [6]), which dictates that the weakest cross section element governs the reduction of the whole cross section. Fulfilment of class 3 conditions for the stiffener itself ensures that there will be no reduction of the stiffener section, and the governing reduction factor results from the global stiffened plate buckling verification. Thus, the difference between the effective cross section method and the reduced stress verification method is not significant. The plate thickness considered ranges from minimum 12 mm to maximum 80 mm (12, 16, 20, 30, 40, 50, 60, 70 and 80 mm, respectively). For the same reason as stated earlier, class 3 condition prohibits the use of all the stiffeners with any plate thickness, so that the ratio $c/t ≤ 42\sqrt{(235/f_y)}$ for the plate in between the stiffener webs can be complied with. The allowed plate thicknesses (t_f) for each stiffener type are also shown in Figure 3.

3. Reduced stress buckling verification – parametric study

3.1. Commentary on provisions from EN 1993-1-5

The method used in this research for buckling verification is based on HRN EN 1993-1-5, Section 10, [6] – reduced stress method. According to the Croatian National Annex for steel bridges (HRN EN 1993-2:2014/NA, Section 2.19, [13]), the reduced stress method is obligatory for buckling verification in ULS or for characteristic combination in SLS. This method limits compression stress in the plate, as opposed to using effective plate section properties [14]. It assumes a linear stress distribution up to the stress limit of the plate element which buckles first [9]. The cross section is fully effective before the limit stress is reached. Thus, all sections are categorized as Class 3 members. For unstiffened plates, this method yields the
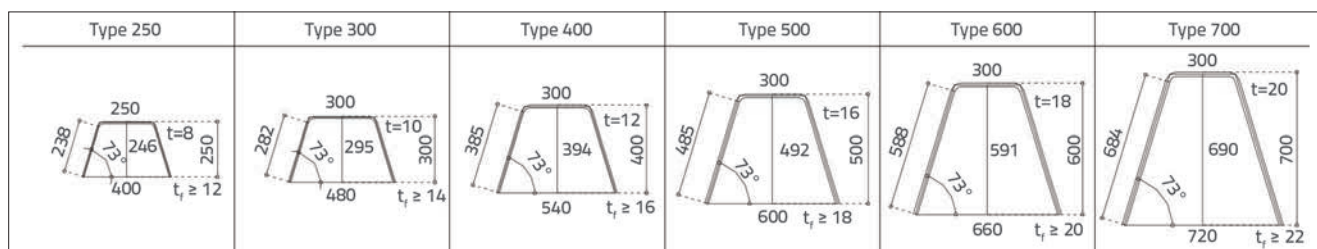

Figure 4. Types of stiffeners developed for the research

same result as does the effective section method. For stiffened plate, the reduced stress method does not take into account redistribution of load from highly stressed to less stressed areas. Because of that, the weakest plate element in the plate governs the design [9]. To overcome this simplification, stiffener types and spacing have been chosen so that all sub plate members satisfy class 3 categorization (as explained in Section 2.2 for stiffener and Section 3.2 for plate thickness). Buckling is verified using the von Mises criterion:

$$\left(\frac{\sigma_{x,Ed}}{\rho_x \cdot f_y / \gamma_{M1}}\right)^2 + \left(\frac{\sigma_{z,Ed}}{\rho_z \cdot f_y / \gamma_{M1}}\right)^2 - \left(\frac{\sigma_{x,Ed}}{\rho_x \cdot f_y / \gamma_{M1}}\right) \cdot \left(\frac{\sigma_{z,Ed}}{\rho_z \cdot f_y / \gamma_{M1}}\right) + 3 \cdot \left(\frac{\tau_{Ed}}{\chi_w \cdot f_y / \gamma_{M1}}\right)^2 \leq 1,0 \quad (2)$$

where $\sigma_{x,Ed}$, $\sigma_{z,Ed}$, τ_{Ed} are design loads, f_y is the yield strength of steel; ρ_x and χ_w are reduction factors, and γ_{M1} is the partial safety factor (for steel in compression, it equals 1.1 in buckling verification according to HRN EN 1993-2:2014/NA, Section 2.19 [13]). For plates in uniaxial compression (compression flanges in box girder bridges), only the first member in equation remains:

$$\left(\frac{\sigma_{x,Ed}}{\rho_x \cdot f_y / \gamma_{M1}}\right)^2 \leq 1,0 \quad (3)$$

Reduction factor is calculated:

$$\rho_x = (\rho - \chi_c)\xi(2 - \xi) + \chi_c \quad (4)$$

where ρ is the reduction due to plate-like behaviour, and χ_c is the reduction due to column-like behaviour of the stiffener. Buckling curve for χ_c is calculated using:

$$\alpha_e = \alpha + \frac{0,09}{i / e} \quad (5)$$

where α = 0,34 (buckling curve b for closed stiffeners), $i = \sqrt{\frac{I_{sl,1}}{A_{sl,1}}}$ $A_{sl,1}$, $I_{sl,1}$ are properties of one stiffener taking into account the adjacent plate width, e is the larger value of the distance between centroid of the stiffener with adjacent plate to the plate centroid or to the centroid of the stiffener without the plate (all according to Figure A.1 contained in HRN EN 1993-1-5 [6]). The interaction factor between these two types of behaviour is:

$$\xi = \frac{\sigma_{cr,p}}{\sigma_{cr,c}} - 1 \quad (6)$$

where $\sigma_{cr,p}$ is the elastic critical plate buckling stress:

$$\sigma_{cr,p} = k_{\sigma,p} \cdot \frac{\pi^2 E}{12(1 - v^2)}\left(\frac{t}{b}\right)^2 \quad (7)$$

$$k_{\sigma,p} \quad \frac{2\left((1 + \alpha^2)^2 + \gamma - 1\right)}{\alpha^2(\psi_x + 1)(1 + \delta)} \text{ za } \lambda \leq \sqrt[4]{\gamma} \quad (8)$$

$$k_{\sigma,p} \quad \frac{4(1 + \sqrt{\gamma})}{(\psi_x + 1)(1 + \delta)} \text{ za } \lambda > \sqrt[4]{\gamma}, \alpha = \frac{a}{b}, \delta = \frac{\sum A_{sl}}{A_p}, \gamma = \frac{I_{sl}}{I_p} \quad (9)$$

where t is the plate thickness; b is the plate width, a is the plate length (4000 mm); ΣA_{sl}, I_{sl} are properties of all stiffeners; A_p, I_p are properties of plate without stiffeners; ψ_x is the edge stress ratio (for pure compression it equals 1.0). $\sigma_{cr,c}$ is the elastic critical column (stiffener) buckling stress:

$$\sigma_{cr,c} = \frac{\pi^2 E I_{sl,1}}{A_{sl,1} a^2} \quad (10)$$

where $A_{sl,1}$, $I_{sl,1}$ are properties of one stiffener considering the plate width according to HRN EN 1993-1-5, Figure A.1 [6]. Reduction factors ρ and χ_w are both calculated according to the relative plate slenderness:

$$\overline{\lambda_p} = \sqrt{\frac{\alpha_{ult,k}}{\alpha_{cr}}} \quad (11)$$

where $\alpha_{ult,k}$ and α_{cr} are minimum load amplifiers to reach the critical resistance and critical elastic load:

$$\frac{1}{\alpha_{ult,k}^2} = \left(\frac{\sigma_{x,Ed}}{f_y}\right)^2 \quad (12)$$

$$\alpha_{cr} = \frac{\sigma_{cr,p}}{\sigma_{x,Ed}} \quad (13)$$

Verification from Equation 3 was used to determine stress limit for each stiffened plate covered in the scope of this research. Adoption of this method is recommended for bridges [7], and Eurocode National Annexes of some countries encourage its use [13].

3.2. Selection of variables – plate width and stiffener arrangement

To complete a parametric study and evaluate the performance of each stiffener, a set of variables must be defined. These variables are: plate width, plate thickness, stiffener type, and stiffener arrangement. Stiffener arrangement is the number of stiffeners distributed along the plate width.

Plate thickness and stiffener type have already been discussed in Section 2.2. As indicated above, the plate thickness ranges from 12 to 80 mm, and possible stiffener type (from 6 preselected types) is chosen for each thickness.

Plate widths were chosen so that they correspond to bridge box sections. In these sections, plate width is determined by the distance between the webs of the box girder (Figure 2), which is dependent on the total bridge width and the number of chambers inside the box girder. For most bridge cross sections of this type, the width ranges from 4 to 10 m (also seen in examples from Figure 1). With the possibility of inclined box girder webs, this range covers any kind of traffic width configuration. Although this research included all widths from 4 to 10 m in 1 m intervals, the results for the widths of 4, 6, 8 and 10 m will be presented in the paper. The widths in between these numbers have been omitted so as to keep the paper within reasonable length limits.
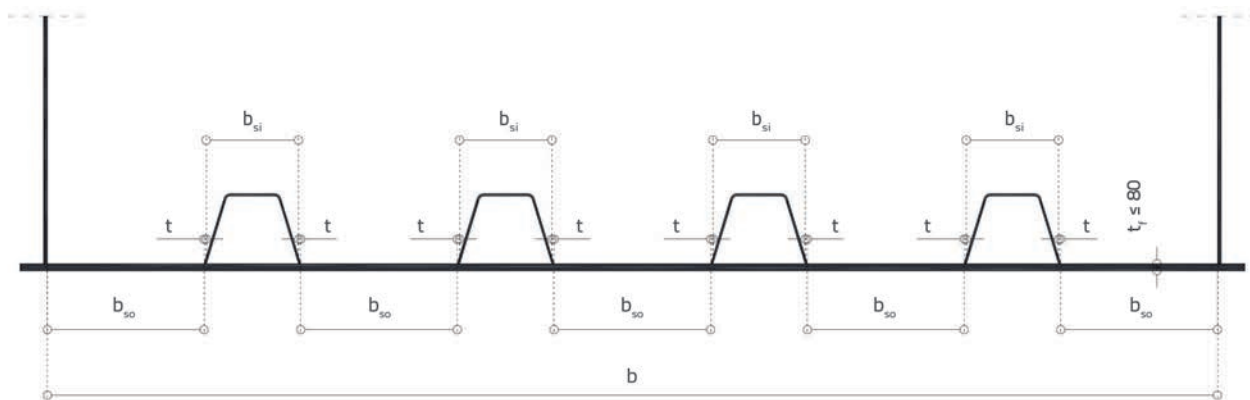
Figure 5. Stiffener arrangement per plate width

The final variable to be considered is the arrangement of stiffeners along the plate width. This arrangement is expressed by the distance between adjacent stiffeners and it defines the total number of stiffeners per plate width. The number of stiffeners is chosen according to following conditions (notations according to Figure 5):

a. Unstiffened part of the plate (part of the plate in between the stiffeners) must fulfil the condition for class 3 sections according to the expression:

$$b_{so} \leq t_f \cdot 42\varepsilon \quad \Rightarrow \quad N_{min} \geq \frac{b - 42\varepsilon \cdot t_f}{42\varepsilon \cdot t_f + b_{si} + 2t} \tag{14}$$

b. Unstiffened part of the plate must be shorter than 1000 mm:

$$b_{so} \leq 1000 \text{ mm} \quad \Rightarrow \quad N_{min} \geq \frac{b - 1000}{1000 + b_{si} + 2t} \tag{15}$$

This condition has been adopted at the author's discretion. In some maintenance scenarios, large box girders need transport of equipment within the section, and so some local loads could occur. The limitation of the unstiffened plate width ensures that these loads can adequately be transferred.

c. A minimum number of 3 stiffeners is adopted ($N_{min} = 3$) for the 4 m plate width.

d. A maximum number of stiffeners is determined in accordance with the requirement that the width of the unstiffened part of the plate in-between stiffeners must correspond to no less than 80 % of the distance between the webs of a single stiffener:

$$b_{so} \geq 0,8 \cdot b_{si} \quad \Rightarrow \quad N_{max} \leq \frac{b - 0,8 \cdot b_{si}}{1,8 \cdot b_{si} + 2t} \tag{16}$$

This condition is also set from experience, so that the algorithm would dismiss the plates with the stiffeners placed too close to one another. Excessively densely placed stiffeners no longer contribute to the buckling resistance.

Conditions a. to d. define boundaries for the possible number of stiffeners for each plate width, plate thickness, and stiffener type. Possible stiffener arrangements according to such conditions are presented in Table 1.

3.3. Parametric presentation of design buckling resistance stresses

The range of stiffened plates has been calculated according to HRN EN 1993-1-5 [6] using parameters described in the previous section. The calculation was performed with an algorithm that increases the design compression stress $\sigma_{x,Ed}$ and verifies Equation 3.

In the verification process, the design compression stress $\sigma_{x,Ed}$ is the product of the loads factored by partial safety factors and combination factors for different simultaneous loading situations, according to the expressions for limit states. Equation (3) dictates that for buckling verification the design

Table 1. Possible number of stiffeners and plate thickness for different plate widths and stiffener types

	Stiffener type (stiffener height in [mm])					
	250	300	400	500	600	700
	Minimal plate thickness [mm]					
	12	16	16	20	20	30
Plate width [m]	Number of stiffeners					
4	3 – 5	3 – 4	3 – 4	3	3	3
6	4 – 7	4 – 6	4 – 5	4 – 5	3 – 4	3 – 4
8	5 – 10	5 – 8	5 – 7	5 – 6	5 – 6	5
10	7 – 13	7 – 11	6 – 9	6 – 8	6 – 7	6 – 7

compression stress must always be equal to or lower than the design buckling resistance of the stiffened plate:

$$\sigma_{x,Ed} \leq \sigma_{red,Rd} = \rho_x \cdot f_y / \gamma_{M1} \tag{17}$$

It is important to remember that the factor ρ_x in Equation (17) is a function dependent on design stress $\sigma_{x,Ed}$. The algorithm records the highest value of $\sigma_{red,Rd}$ for which Equation 17 is satisfied for each plate. Results are plotted on charts (Figure 6 – Figure 9) for plates 4, 6, 8 and 10 m in width. These charts show the design compression stress under which each of the stiffened plates, according to its thickness, satisfies the buckling verification with full utilization $\sigma_{x,Ed} / (\rho_x \cdot f_y / \gamma_{M1}) = 1,0$. This stress can also be called the design buckling resistance stress.
Each curve in the chart represents a different stiffener type and configuration (number of stiffeners). A curve is added in the chart to show results for a plate without stiffeners (according to the example shown in [15]). Each chart also shows the maximum design compression stress when no buckling is possible. A discontinuity in curves can be observed on a 40 mm mark due to change in the yield strength of the steel. In smaller-width plates with smaller stiffeners, there is an increase in the design

buckling resistance as they get thicker, because the interaction factor for the plate and column type buckling behaviour (ξ in Equation 6) is larger, influencing the plate-like behaviour that becomes more prominent. This is particularly visible when the thickness approaches 80 mm.

4. Stiffened plate optimization process

4.1. Shear lag consideration

Optimization charts developed in Section 4.2 show the area of the stiffened plate that is needed for any design compression force in the flange, and stiffener type. The design compression force in the flange is calculated according to the previously shown design resistance stress $\sigma_{red,Rd}$:

$$F = A_{fs} \cdot \beta \cdot \sigma_{red,Rd} \tag{18}$$

where A_{fs} is the total area of the plate with stiffeners, β is the reduction due to shear lag and $\sigma_{red,Rd}$ is the design resistance stress under which buckling occurs. The reduction due to shear lag from
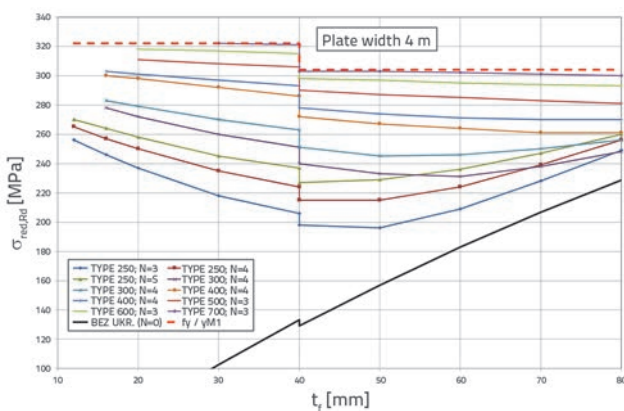

Figure 6. Design buckling resistance stress for stiffened plates 4 m in width
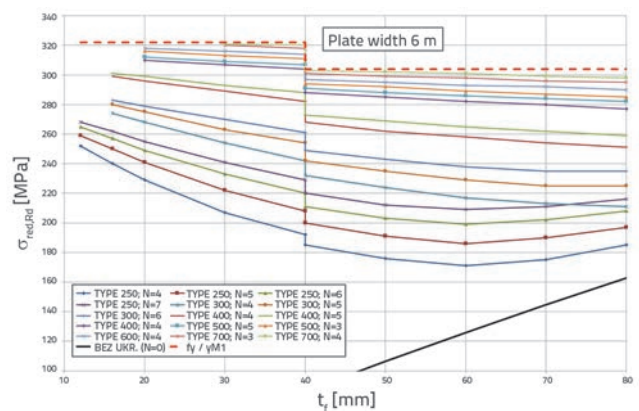

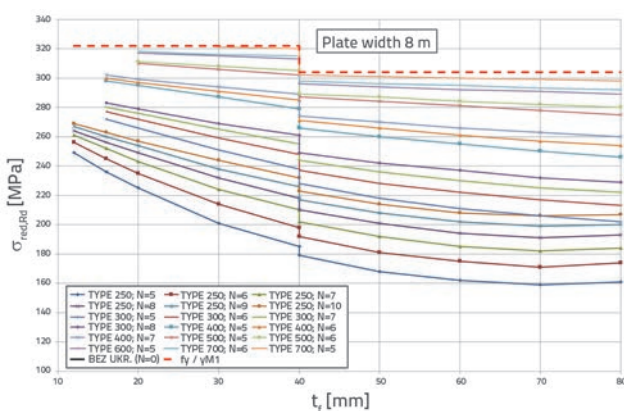Figure 7. Design buckling resistance stress for stiffened plates 6 m in width

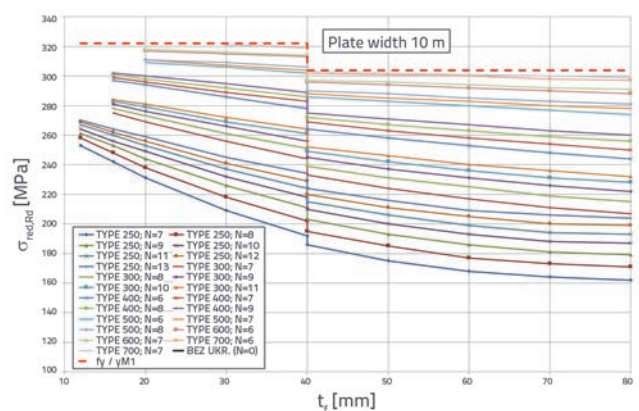Figure 8. Design buckling resistance stress for stiffened plates 8 m in width

Figure 9. Design buckling resistance stress for stiffened plates 10 m in width

the negative hogging bending moment (which causes compression in the bottom flange) is dependent on the effective length, plate width, and stiffener to plate area ratio (stiffener contribution):

$$\beta = \frac{1}{1+6\left(\kappa - \frac{1}{2500\kappa}\right)+1{,}6\kappa^2}, \ \kappa = \alpha_0 b_0 \,/\, L_e, \ \alpha_0 = \sqrt{1+\frac{A_{sl}}{b_0 t}} \qquad (19)$$

where:
A_{sl} - the area of stiffeners
b_0 - one half of the plate width
L_e - the effective length
α_0 - he coefficient that takes into account stiffener contribution to shear lag.

If the compression force calculated in Equation 18 is to be made independent of the shear lag factor β, then the charts from Section 4 would be applicable to any bridge, regardless of its span. But, in such a case, curves that show the steel area needed for each stiffened plate, and are derived for different types and configuration of stiffeners, would not be comparable, since shear lag is dependent on the stiffener to plate ratio (α_0). Plates of the same width, and for same effective length, can still have different shear lag reduction factors because of different stiffener configurations. Thus, the optimization in finding the minimum surface among these plates for the same compression force would not be correct. The ideal solution for this problem would be to break the shear lag reduction factor β into two parts – shear lag reduction that comes from plate width and effective length ratio (β'), and the other part that comes from the stiffener to plate ratio (α'):

$$\beta = f(\kappa) = f(\alpha_0, b_0, L_e) = f(\alpha_0)\cdot f(b_0, L_e) = \alpha'\cdot\beta' \quad \Rightarrow \quad \alpha' = \frac{\beta}{\beta'} \ (20)$$

In Equation 20, β' is the shear lag reduction factor calculated with $\kappa = b_0/L_e$ that doesn't take into account the stiffener to plate area ratio. Looking at Equation 19, it is clear that solution for α' is not possible as an analytically exact solution. To overcome this problem, a study of values β, α' and β' was made to see how they change with α_0, b_0 and L_e. For the selected plates and

stiffeners, α_0 ranges from 1.02 to 1.43, while b_0 and L_e ranges were taken as explained in Section 3.2. The results of this study are shown in Table 2.

The goal of the study from Table 2 was to find the constant effective length that would be used in further calculation of α' according to Equation 20. The condition for choosing the constant L_e is that the difference between the reduction α', derived with this L_e, and the reduction α' derived with the smallest and largest L_e, be minimal. All reductions were calculated for possible cases of α_0 (α_0 = 1.0 do 1.43), and possible cases of plate widths (b_0 = 2 to 5 m). The value L_e that satisfies this condition the best is 66 m, with an error of up to 4.37 %. Larger error of 6.89 % occurs only when the shear lag reduction β' (reduction for plate without the stiffener when α_0 = 1.0) equals 1.0, which is the case when the effective lengths are large. Such cases are not common when the bottom flange is compressed (cross sections above supports with hogging bending moments). According to results from Table 2, an effective length of 66 m was adopted for all further calculations. The compression force from Equation 18 can now be written:

$$F = A_{fs}\cdot\beta'\cdot\alpha'(L_e = 66\ m)\cdot\sigma_{red,RD} \qquad (21)$$

$$F_\beta = \frac{F}{\beta'} = A_{fs}\cdot\alpha'(L_e = 66\ m)\cdot\sigma_{red,Rd} \qquad (22)$$

Calculated in this way, the compression force F_β is no longer dependent on the effective length for the shear lag effect, but still takes into account the effects of the stiffener area on shear lag reduction. Thus, charts from Section 4 are comparable for the same compression force F_β and can be used for any effective length. As discussed, a minor error of no more than 4.37 % (when the effective lengths are minimal, i.e. 40 m) was adopted to make this possible.

4.2. Algorithm for optimization chart plotting

The stiffened plate is subjected to the design compression force. In high box girders, as in bridges, it can be adopted that the compression stresses due to this force are distributed to stiffeners along their height [9]. The accuracy of this approximation increases with the reduction of the stiffener to section height ratio. Thus,

Table 2. Parametric study of shear lag reduction

b_0	2			5		
L_e	40	66	130	40	66	130
	β					
α_0 = 1.02	0.792	0.901	1.0	0.564	0.693	0.85
α_0 = 1.43	0.712	0.828	0.977	0.474	0.607	0.774
	β'					
α_0 = 1.0	0.796	0.906	1.0	0.57	0.698	0.854
	$\alpha' = \beta\,/\,\beta'$					
α_0 = 1.02	0.995	0.994	1.0	0.989	0.993	0.995
α_0 = 1.43	0.894	0.914	0.977	0.831	0.869	0.906
	ERROR for α': [$\alpha'(L_e$ = 66 m)- α'] / $\alpha'(L_e$ = 66 m)					
α_0 = 1.43	2.19 %	0 %	-6.89 %	4.37 %	0 %	-4.26 %

the total maximum compression force in the stiffened plate is assumed by both, the plate and the stiffeners. These stresses act on the effective width of the stiffened plate. The maximum design compression force, before buckling, can be calculated using Equation 18, or Equation 22 when omitting a part of shear lag due to effective span length, as described in Section 4.1.

For each plate from Section 3.3, the algorithm calculates the area A_{fs} and the reduction factor α' and, finally, the compression force F_β. The algorithm also records the total area of the stiffened plate. This area represents the steel quantity needed to take on compression force, and as such is one of the parameters used for optimization. Charts presented in Figures 10 to 13 were plotted using the data from the algorithm. These charts show the steel area needed for each stiffened plate width. Each chart contains curves representing the number and types of stiffeners. Additional curves are added that connect the graph points of the plates of similar thickness (trend lines). Intermediate thicknesses can be approximated by graphical interpolation of these curves. Each point on the plotted curves shows the allowed design compression force and the total steel area for a specific type and number of stiffeners, for each plate width on a separate chart.

4.3. Interpretation of charts and optimization criteria

As expected, chart curves (Figures 10 to 13) representing thicker plates are higher in the chart area. Curves for plates with stronger stiffeners, or a larger number of stiffeners are further to the right in the chart area (larger design compression force allowed). Curves for plates with weaker stiffeners end sooner in the chart area (lesser design compression force possible). For comparison, a curve is plotted in each chart representing the unstiffened plate.

The values of design compression force that can be assumed by a specific stiffened plate are mainly dependent on its area and so, naturally, wider plates reach higher maximum values within the charts. Interestingly, curves for smallest stiffeners (Type 250) and largest stiffeners (Type 600 and Type 700) are relatively close to each other in case of stiffened plates 4 m in width, which means that the plate areas needed to assume the same compression force do not differ by much for different stiffener types. This is especially noticeable for larger values of plate compression force, or for greater plate thicknesses. For example, for the 90 MN compression force, the smallest-area plate that meets the stability requirements is the plate type 700 t = 50 mm, while the corresponding greatest-area plate is the plate type 250 t = 70 mm. The difference between these two areas is 11 % only. For comparison, in a 6 m wide plate and for the same compression force, the smallest-area plate meeting the stability requirements (Type 700 t = 30 mm) and the corresponding greatest-area plate (Type 250 t = 70 mm) differ by as much as 66 % in area. Even larger differences can be observed for the plates 8 m and 10 m in width. This can be explained by interaction of the plate-like and column-like behaviour during buckling (Equation 4). For wider plates, the interaction factor ξ (Equation 6) is either 0 or is very small, meaning that the buckling is realized via the stiffener

column failure. For narrower plates (especially noticeable in plates 4 m in width) and thicker plates, the interaction factor ξ is larger – as large as 0,353 for plates with the weaker type 250 stiffeners. In these cases, because of the plate-like behaviour, the stress reduction due to buckling is much smaller, which is also visible in Figure 6 (ascending part of the type 250 and type 300 curves for rising plate thickness). For wider plates, an increase in plate thickness will not have such an effect on the increase in the design buckling resistance stress. This increase can then be achieved only by increasing the stiffness (height) of the stiffener itself. Therefore it is always more rational to use thinner plates and higher stiffeners for wider plates, as can clearly be seen from the charts.

Finally, these charts can be used to perform optimization in order to define the best stiffener type and number according to the acting compression force, for each plate width. Optimization criteria were adopted to favour certain plate thickness, stiffener type and number of stiffeners, as follows:

a. stiffened plates with the least steel area are chosen first (steel consumption condition),

b. when several stiffened plates are of the same area (curves overlapping or close to one another), the plate with a lower number of stiffeners is chosen (steel workshop time condition).

Plates that meet these criteria are shown below the chart area depending on the value of compression force. They are the result of the bottom (lowest) envelope of curves data, and can be considered optimal with regard to the buckling verification code HRN EN 1993-1-5 [6]. It can be observed that compliance with the above conditions also means that the optimal chosen plate will have the smallest possible thickness that is associated with a higher stiffener. With higher stiffeners, a smaller number of stiffeners results in a more favourable plate because of the smaller shear lag reduction (due to the more favourable stiffener to plate ratio).

5. Application

Two sets of charts presented in this research are applicable to steel box girder bridges with stiffened compression bottom flanges. The first set of charts (Section 3.3) reveals the design buckling resistance that is compliant with HRN EN 1993-1-5, Section 10 [6] for a range of stiffeners, plate thicknesses, and plate widths. Stiffener types used in this research cover most heights and shapes that are commonly used in bridges, while stiffeners of greater height are added for larger scope of application. These charts can be used in the design to quickly determine if the chosen plate with stiffeners of the same of similar characteristics and configuration as the ones in the charts can withstand the design compression stress without buckling. If not, then a stiffener type and configuration satisfying the required design stresses can be chosen for the same plate thickness.

The second set of charts (Section 4.3) can be used to select an optimum stiffening solution. For a given section of a box girder
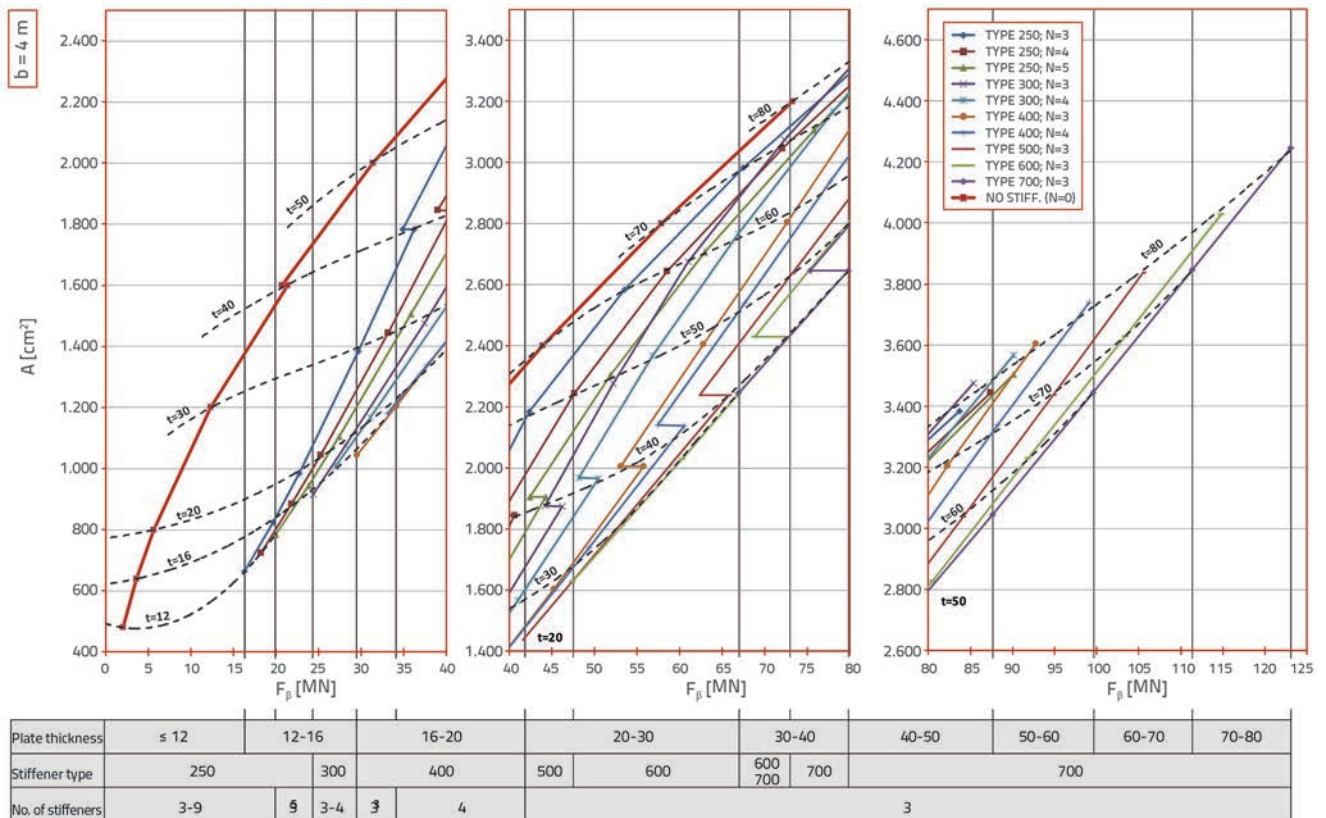
Plate thickness	≤ 12	12-16	16-20	20-30	30-40	40-50	50-60	60-70	70-80
Stiffener type	250	300	400	500	600	600 700	700		700
No. of stiffeners	3-9	5	3-4 3	4			3		

Figure 10. Optimization chart for stiffened plates 4 m in width

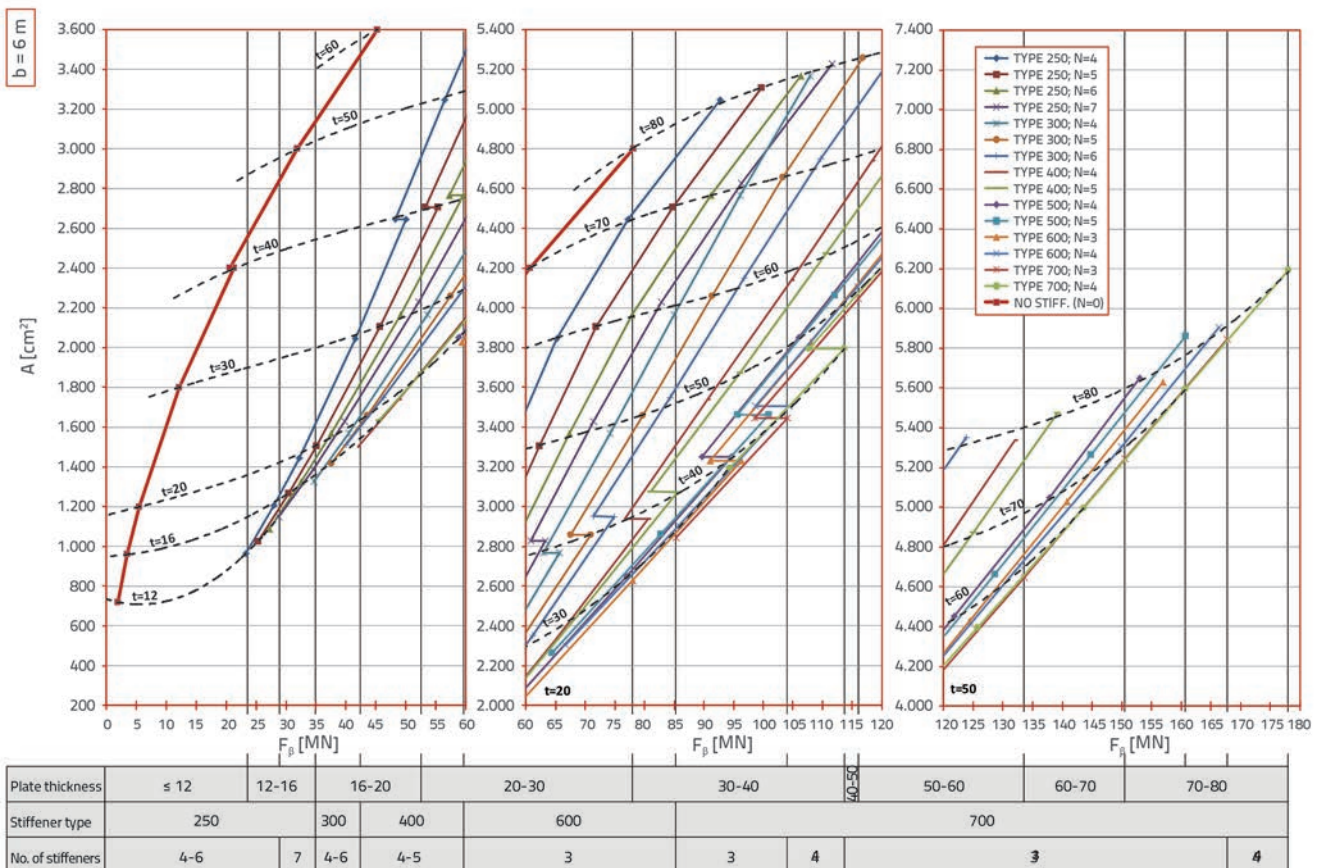| Plate thickness	≤ 12	12-16	16-20	20-30	30-40	40-50	50-60	60-70	70-80
Stiffener type	250	300	400	600			700		
No. of stiffeners	4-6	7	4-6 4-5	3	3 4		3		4

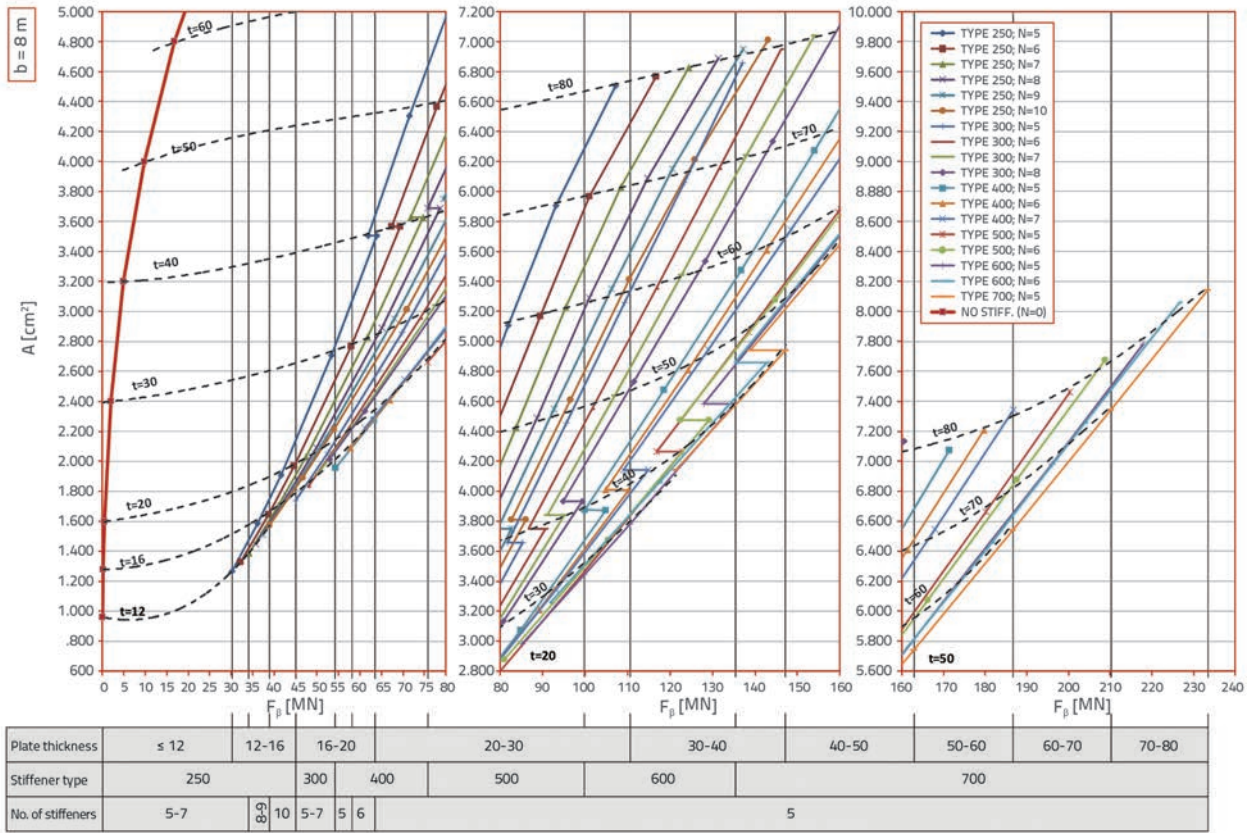**Figure 11. Optimization chart for stiffened plates 6 m in width**

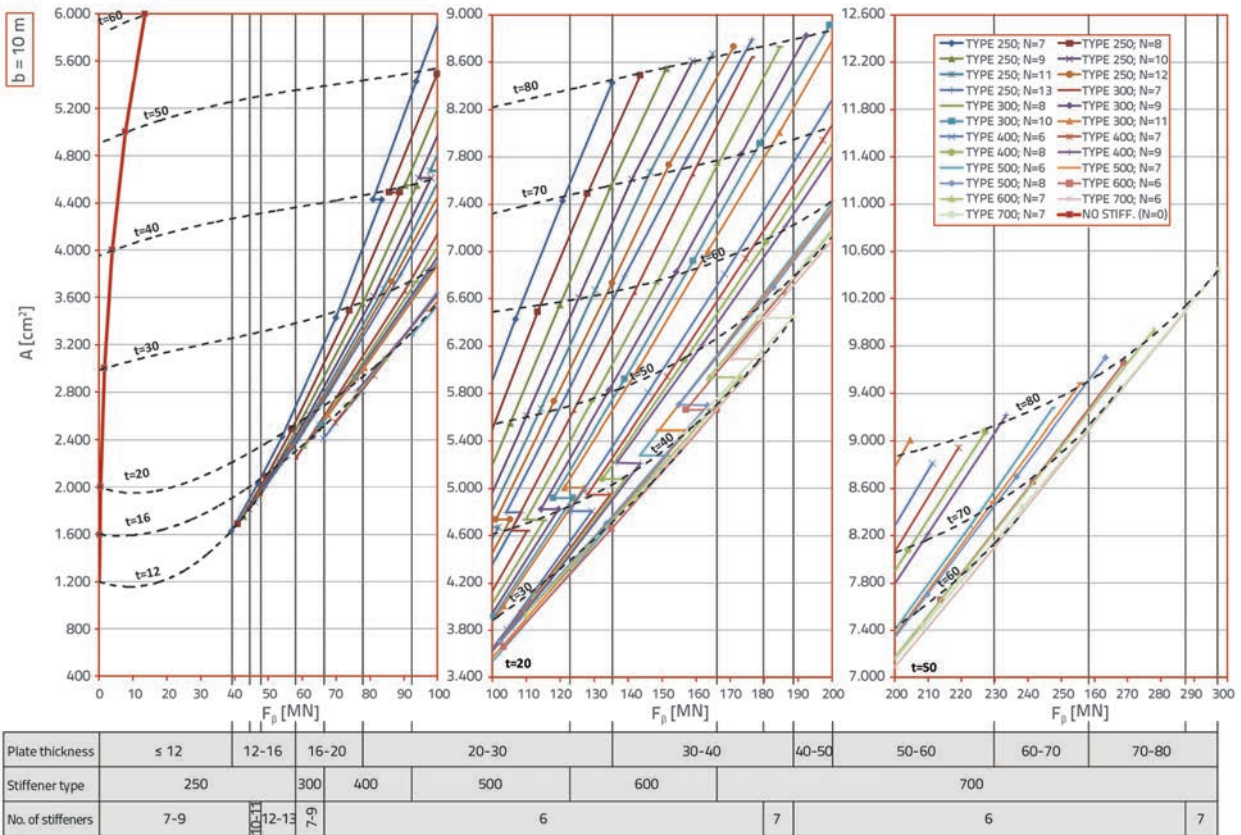**Figure 12. Optimization chart for stiffened plates 8 m in width**

Figure 13. Optimization chart for stiffened plates 10 m in width

bridge (with a presumed bottom flange plate) and the acting design bending moment, a compression force in the bottom flange can be approximated from static properties of the girder box section. In the first iteration, it is recommended that this force be approximated as a larger one, considering the earlier-adopted assumption that the stresses are distributed evenly along the stiffener height (cf., Section 4.2). Since this is not exactly true, especially in box girders of smaller height, the approximation of larger force will ensure a more accurate reading from the optimization chart. Furthermore, this compression force is then divided by the shear lag reduction factor β (using the coefficient α_o=1.0 because this coefficient has already been considered in the charts), which results in an increased compression force F_β. Using an appropriate chart (according to plate width), the optimal stiffened plate (defined by thickness, stiffener type, and number of stiffeners) can then be chosen for the compression force F_β. This procedure is to be iterated by updating box section properties with the newly chosen stiffened plate from the previous step, and deriving an updated compression force in bottom flange from bending. When the plate thickness and stiffeners are known from the first iteration, the compression force can be determined more accurately from the stresses in the bottom flange and compared once again to the chart values. The iterations finish when both the compression force and stiffening solution match the information from optimization table in the chart. Since the compression force in a flange of high box girder

sections does not change by much when changing the flange plate thickness and stiffeners, the iteration process converges rapidly and an optimum plate can quickly be determined. These charts can also be used if compression forces F_β, and plate thickness are known. The curve closest to the point in the chart defined by these variables then represents the required stiffener type and number for such a plate.

6. Conclusion

Results of this research can be used for a stiffened compression plate in bridge box girders with the plates 4 m in length (typical distance between section cross girders or diaphragms). Derived charts showing the design buckling resistance stresses can also be applied to any other structure with similar dimensions and loads in compression plates. Using the results from this research, the stiffening solution that best satisfies the buckling verification according to HRN EN 1993-1-5 can quickly be reached and can be considered optimal with regard to the steel consumption and workshop time. The stiffening solution implies selection of 6 types of stiffeners with different height and thickness, number of stiffeners, and the selection of plate thickness. The final buckling verification performed on a plate chosen according to charts and guidelines from this paper will result in a full utilization of the plate, and hence in an optimum plate stiffening solution.

REFERENCES

[1] Mensinger, M., Ndogmo, J., Parra, R.: Optimization of stiffened plates for steel bridges based on Eurocode 3 Part 1-5 using genetic algorithms, STEEL CONSTRUCTION, 4 (2011) 1, pp. 29-33, https://doi.org/10.1002/stco.201110005

[2] Kaveh, A., Bakhshpoori, T., Barkhori, M.: Optimum design of multi-span composite box girder bridges using Cuckoo Search algorithm, Steel and Composite Structures, 17 (2011) 5, pp. 705-719.

[3] Unterweger, H., Lechner, A., Greiner, R.: Plastic load bearing capacity of multispan composite highway bridges with longitudinally stiffened webs, Steel and Composite Structures, 11 (2011) 1, pp. 1-19, https://doi.org/10.12989/scs.2011.11.1.001

[4] Ferreira, P., Virtuoso, F.: Stiffened flanges used in steel box girder bridges, International Conference on Multi-Span Large Bridges, Porto, Portugal, July 2015, https://doi.org/10.1201/b18567-151

[5] Maiorana, E., Pellegrino, C.: Linear buckling analysis of welded girder webs with variable thickness, Steel and Composite Structures, 11 (2011) 6, pp. 505-524, https://doi.org/10.12989/scs.2011.11.6.505

[6] HRN EN 1993-1-5:2006 Eurokod 3 Projektiranje čeličnih konstrukcija, dio 1-5: Pločasti konstrukcijski elementi (EN 1993-1-5:2006+AC:2009), Hrvatski zavod za norme, Zagreb, Hrvatska, 2014.

[7] Naumes, J., Feldmann, M., Sedlacek, G.: Demonstration of the common basis of method 1 (effective width approach) and method 2 (stress limit approach) for the plate-buckling assessment of built-up steel components according to Eurocode 3-Part 1-5, Stahlbau, 78 (2009) 3, pp. 139-147, https://doi.org/10.1002/stab.200910014

[8] HRN EN 1993-1-1:2014 Eurokod 3 Projektiranje čeličnih konstrukcija, dio 1-1: Opća pravila i pravila za zgrade (EN 1993-1-1:2005+AC:2009), Hrvatski zavod za norme, Zagreb, Hrvatska, 2014.

[9] Beg, D., Kuhlmann, U., Davaine, L., Braun, B.: Design of Plated Structures, ECCS – European Convention for Constructional Steelwork, Ernst & Sohn, Berlin, Germany, 2010.

[10] Grondin, G.Y., Elwi, A.E., Cheng, J.J.R.: Buckling of stiffened steel plates – a parametric study, Journal of Constructional Steel Research, 50 (1999), pp. 151-175, https://doi.org/10.1016/S0143-974X(98)00242-9

[11] Sheikh, I.A., Elwi, A.E., Grondin, G.Y.: Stiffened steel plates under uniaxial compression, Journal of Constructional Steel Research, 58 (2002), pp. 1061-1080, https://doi.org/10.1016/S0143-974X(01)00083-9

[12] Mittelstedt, C.: Explicit analysis and design equations for buckling loads and minimum stiffener requirements of orthotropic and isotropic plates under compressive load braced by longitudinal stiffeners, Thin-Walled Structures, 46 (2008), pp. 1409-1429, https://doi.org/10.1016/j.tws.2008.03.007

[13] HRN EN 1993-2:2014/NA Eurokod 3 Projektiranje čeličnih konstrukcija, dio 2: Čelični mostovi – Nacionalni dodatak, Hrvatski zavod za norme, Zagreb, Hrvatska, 2014.

[14] Galéa, Y., Martin, P.-O.: Longitudinally stiffened plates in Eurocode 3: Calculation of the global critical buckling stress, Journal of Constructional Steel Research, 66 (2010), pp. 1345-1353, https://doi.org/10.1016/j.jcsr.2010.05.001

[15] Unterweger, H., Kettler, M.: Unstiffened panels - Really big differences between Eurocode EN 1993-1-5 and DIN 18800-3, Stahlbau, 82 (2013) 8, pp. 557–634.